Mechanotaxis directs *Pseudomonas aeruginosa* twitching motility

Marco J. Kühn[a,b,1], Lorenzo Talà[a,b,1], Yuki F. Inclan[c], Ramiro Patino[c], Xavier Pierrat[a,b], Iscia Vos[a,b,d], Zainebe Al-Mayyah[a,b], Henriette Macmillan[c], Jose Negrete Jr[a,b,d], Joanne N. Engel[c,e,2], and Alexandre Persat[a,b,2]

[a]Institute of Bioengineering, School of Life Sciences, École Polytechnique Fédérale de Lausanne, CH-1015 Lausanne, Switzerland; [b]Global Health Institute, School of Life Sciences, École Polytechnique Fédérale de Lausanne, CH-1015 Lausanne, Switzerland; [c]Department of Medicine, University of California, San Francisco, CA 94143; [d]Institute of Physics, School of Basic Sciences, École Polytechnique Fédérale de Lausanne, CH-1015 Lausanne, Switzerland; and [e]Department of Microbiology and Immunology, University of California, San Francisco, CA 94143

Edited by Dianne K. Newman, California Institute of Technology, Pasadena, CA, and approved June 10, 2021 (received for review January 28, 2021)

The opportunistic pathogen *Pseudomonas aeruginosa* explores surfaces using twitching motility powered by retractile extracellular filaments called type IV pili (T4P). Single cells twitch by sequential T4P extension, attachment, and retraction. How single cells coordinate T4P to efficiently navigate surfaces remains unclear. We demonstrate that *P. aeruginosa* actively directs twitching in the direction of mechanical input from T4P in a process called mechanotaxis. The Chp chemotaxis-like system controls the balance of forward and reverse twitching migration of single cells in response to the mechanical signal. Collisions between twitching cells stimulate reversals, but Chp mutants either always or never reverse. As a result, while wild-type cells colonize surfaces uniformly, collision-blind Chp mutants jam, demonstrating a function for mechanosensing in regulating group behavior. On surfaces, Chp senses T4P attachment at one pole, thereby sensing a spatially resolved signal. As a result, the Chp response regulators PilG and PilH control the polarization of the extension motor PilB. PilG stimulates polarization favoring forward migration, while PilH inhibits polarization, inducing reversal. Subcellular segregation of PilG and PilH efficiently orchestrates their antagonistic functions, ultimately enabling rapid reversals upon perturbations. The distinct localization of response regulators establishes a signaling landscape known as local excitation–global inhibition in higher-order organisms, identifying a conserved strategy to transduce spatially resolved signals.

type IV pili | mechanosensing | chemotaxis | twitching | motility

Single-cell organisms have evolved motility machineries to explore their environments. For example, bacteria utilize swimming motility to propel themselves through fluids. In their natural environments, bacteria are, however, most commonly found associated to surfaces (1). Many species use surface-specific motility systems such as twitching, gliding, and swarming to migrate on solid substrates (2). However, we still know very little about how cells regulate and control surface motility. In particular, the role of mechanical signals in regulating the motility of single cells remains vastly underexplored in bacteria as well as in higher-order microorganisms (3).

To migrate toward nutrients and light or away from predators and toxins, cells actively steer motility in response to environmental signals. For example, chemotactic systems mediate motility toward specific molecular ligands (4, 5). Bacteria have a remarkably diverse set of chemotaxis systems. The canonical Che system, which has been extensively studied as a regulator of *Escherichia coli* swimming, is widely conserved among motile species including nonswimming ones (6). However, the signal inputs and the motility outputs of other bacterial chemotaxis-like systems remain incompletely understood in many species (7). Finally, chemotaxis-like systems are found with alternative signaling architectures, including additional components compared with the Che system. For example, while Che controls flagella rotation by phosphorylation of a single response regulator, other species can use up to six. The functions of these supplementary elements remain cryptic (8).

Pseudomonas aeruginosa is a major opportunistic pathogen well adapted to growth on surfaces. *P. aeruginosa* colonizes and explores abiotic and host surfaces using twitching motility, which is powered by retractile extracellular filaments called type IV pili (T4P) (9). During twitching, single cells pull themselves by successive rounds of T4P extension, attachment, and retraction (9, 10). T4P extend and retract from the cell surface by respective polymerization and depolymerization of the pilin subunit PilA at the poles (9, 10). While an understanding of the assembly mechanisms of individual filaments is beginning to emerge, we still do not know whether and how cells coordinate multiple T4P to power migration over large distances.

Genetic studies show that a chemotaxis-like system called Chp regulates twitching (11). Beyond playing a role in the transcription of T4P genes, the mechanism by which Chp regulates motility remains unknown (12, 13). Also, unlike Che, which possesses a single response regulator, the Chp system possesses two response regulators, PilG and PilH, whose respective functions and mechanism of action are incompletely resolved (14) (Fig. 1*A*). Most Chp mutants twitch aberrantly most often because of the downregulation of T4P machinery, making their motility phenotypes

Significance

Single cells across kingdoms of life explore, prey, escape, or congregate using surface-specific motility. Motile eukaryotic cells use chemotaxis to direct migration on surfaces. However, how bacteria control surface motility remains underexplored. *Pseudomonas aeruginosa* twitches on surfaces by successive extension and retraction of extracellular filaments called type IV pili. Here, we show that *P. aeruginosa* directs twitching by sensing mechanical input generated by type IV pili. The Chp sensory system performs spatially resolved mechanosensing by harnessing two response regulators with antagonistic functions. Our results demonstrate that sensory systems, whose input often remains elusive, can sense mechanical signals to actively steer motility. Furthermore, Chp establishes a signaling principle shared with higher-order organisms, identifying a conserved strategy to transduce spatially resolved signals.

Author contributions: M.J.K., L.T., J.N.E., and A.P. designed research; M.J.K., L.T., and Y.F.I. performed research; M.J.K., L.T., I.V., R.P., Y.F.I., X.P., Z.A.-M., J.N., and H.M. contributed new reagents/analytic tools; M.J.K., L.T., and I.V. analyzed data; and M.J.K., L.T., J.N.E., and A.P. wrote the paper.

The authors declare no competing interest.

This article is a PNAS Direct Submission.

[1]M.J.K. and L.T. contributed equally to this work.

[2]To whom correspondence may be addressed. Email: joanne.engel@ucsf.edu or alexandre.persat@epfl.ch.

This article contains supporting information online at https://www.pnas.org/lookup/suppl/doi:10.1073/pnas.2101759118/-/DCSupplemental.

Published July 22, 2021.

hard to interpret (11). In addition, unlike homologs from the well-studied canonical *E. coli* Che system, the Chp methyl-accepting chemotaxis protein called PilJ has no clear chemical ligand (13, 14). Several chemical compounds bias collective or single-cell twitching migration in a Chp-dependent manner (15–18). For example, single *P. aeruginosa* cells twitch up strong gradients of dimethyl sulfoxide (17). Because most Chp mutants have strong piliation defects, it remains unclear whether chemical gradients passively bias twitching displacements or actively guide motility via chemosignaling.

We previously demonstrated that *P. aeruginosa* up-regulates genes coding for virulence factors upon surface contact in a T4P- and Chp-dependent manner (13, 19). However, how Chp controls motility independently of transcription remains unresolved (11, 13, 20). The homology between Chp and Che systems suggests a tactic function for Chp. As a result, we rigorously tested the hypothesis that Chp regulates twitching motility of single cells in response to T4P mechanical input at short timescales.

Results

The canonical Che system regulates bacterial swimming by transducing an input chemical signal into a motility response via flagellar rotation control (21). By analogy, we hypothesized that the chemotaxis-like Chp system regulates the trajectory of single twitching cells (13). Chp mutants twitch aberrantly in the traditional stab assay (*SI Appendix*, Fig. S1 *A* and *B*) (12, 20). These

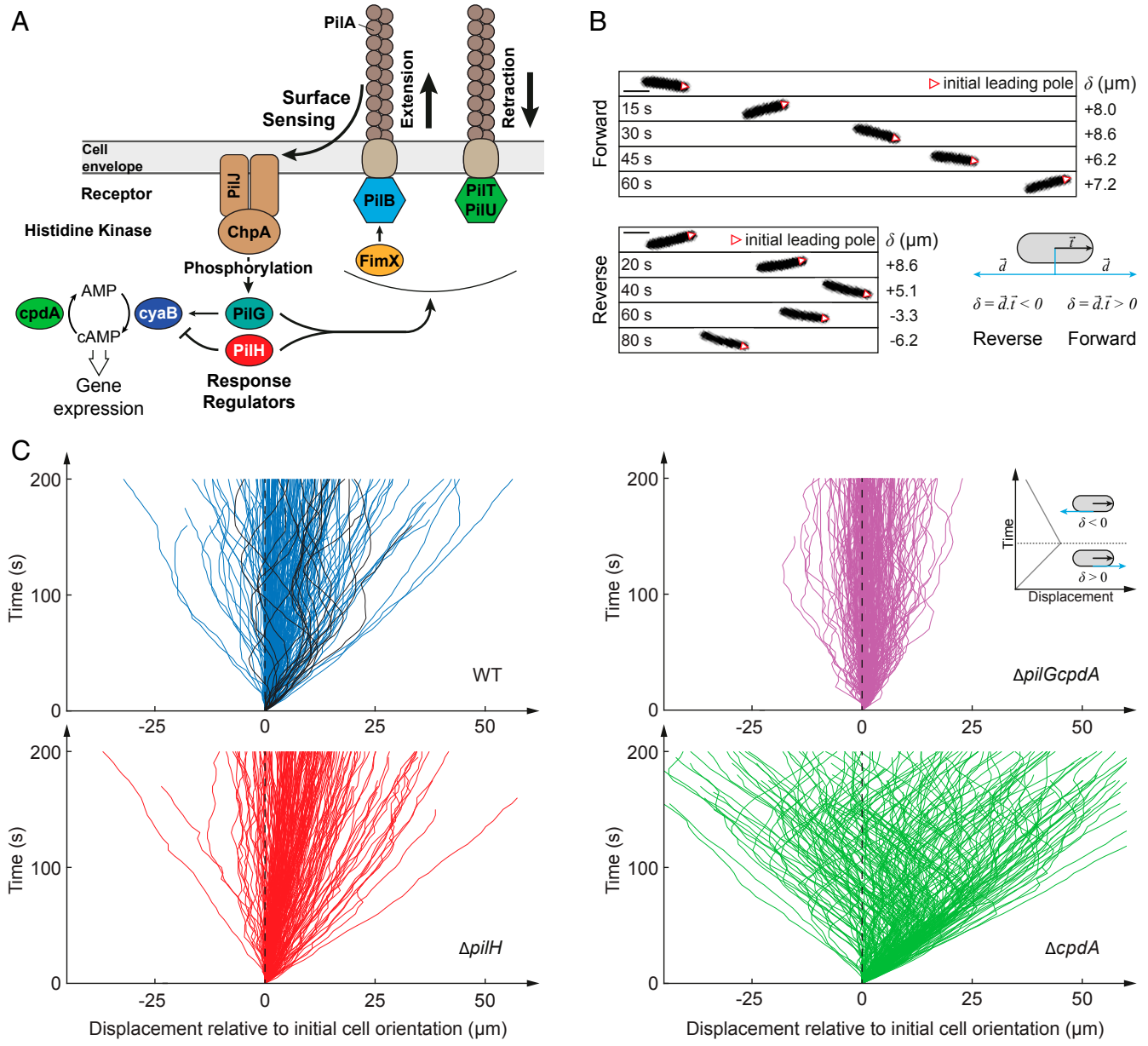

Fig. 1. The Chp system regulates the twitching trajectories of individual *P. aeruginosa* cells. (*A*) Schematic representation of the major components of the T4P and Chp system. (*B*) Phase contrast snapshots of forward and reverse migration of twitching cells. $\vec{t}$ is a unit vector oriented along the cell body in the initial direction of motion. $\vec{d}$ is the unit displacement vector. δ is the dot product $\vec{d}.\vec{t}$, which quantifies displacements relative to the initial direction of motility. The red triangle indicates the initial leading pole of the bacterium. (Scale bar, 2 μm.) (*C*) Graphs of cumulative net displacement as a function of time, highlighting the forward and reverse twitching behavior of Chp mutants. Each curve corresponds to an individual cell trajectory. Tracks of reversing WT cells are highlighted in black. At any given time, a curve oriented toward the top right corresponds to a cell moving forward, while a curve oriented toward top left corresponds to reverse movement (*cf. Inset*). Δ*pilGcpdA* constantly reverses twitching direction, while Δ*pilH* cells persistently move forward.

mutants also have altered cyclic AMP (cAMP) levels (*SI Appendix*, Fig. S1*C*) (19). cAMP regulates the transcription of virulence genes upon surface contact so that Chp mutants have aberrant T4P numbers (*SI Appendix*, Fig. S1*D*) (19). To overcome a potential crosstalk, we decoupled the Chp-dependent, short timescale motility control from cAMP-dependent transcription by investigating single-cell twitching in constitutively low or high cAMP regimes.

We first explored the functions of Chp in directing twitching motility by visualizing individual isolated motile wild-type (WT) (Fig. 1*B* and Movie S1), Δ*cpdA*, Δ*pilH*, and Δ*pilGcpdA* cells at the interface between a glass coverslip and an agarose pad. For these strains, which all have elevated cAMP levels (*SI Appendix*, Fig. S1*C*), we computed the linear displacements of single cells to visually highlight the balance between persistent forward motion and reversals for single cells (Fig. 1*C*). We also computed their mean reversal frequency (Fig. 2*A*). WT and Δ*cpdA* cells mostly move persistently forward and only occasionally reversed twitching direction (Figs. 1*C* and 2*A*). Δ*pilGcpdA* cells reversed so frequently that they appeared to "jiggle," never committing to a single direction of twitching (Figs. 1*C* and 2*A* and Movie S2). They ultimately had very little net migration, consistent with their reduced twitching motility in the stab assay (*SI Appendix*, Fig. S1*A*). By contrast, Δ*pilH* moved very persistently in a single direction and reversed very rarely (Figs. 1*C* and 2*A*). Likewise, Δ*pilHcyaB*, which has reduced cAMP levels compared with Δ*pilH*, had near zero reversal frequency, confirming the Chp-dependent, cAMP-independent control of twitching direction (Fig. 2*A*).

WT cells often reversed their twitching direction after a side collision (Fig. 2 *B* and *C* and Movie S3). Δ*pilGcpdA* reversed almost always after impact, whereas Δ*pilH* almost never did (Fig. 2 *B* and *C* and Movie S3). This suggests that cell–cell contact may mechanically interrupt Chp signaling at the colliding pole or that Chp chemically senses the surface of the other cell. To distinguish between these hypotheses, we inspected how cells reversed upon collisions with nonbiological material. We produced micrometer-wide glass microfibers that we added to the twitching environment, thereby producing obstacles to the motile bacteria. Upon colliding these microfibers, WT cells often reversed twitching direction (Fig. 2*D* and Movie S4). The rate of reversal upon colliding glass was indistinguishable from collisions with other cells (Fig. 2*E*). These observations are therefore consistent with a mechanism in which cell–cell contact mechanically perturbs Chp signaling.

The Chp-dependent control of reversal rates is reminiscent of the role of the Frz sensory system in controlling motile collective behavior in *Myxococcus xanthus* (22, 23). We therefore explored how mutations in Chp influenced group motility. At high cell density, WT cells spread relatively evenly over the surface (Fig. 2*F*). In contrast, collision-blind Δ*pilH* cells jammed head to head, forming small groups that inefficiently moved forward (Fig. 2*F* and Movie S5). At a much higher cell density, in a WT colony, the bacteria distribute evenly across the field of view and form persistent rafts at the leading edge, thereby expanding the colony edge rapidly (*SI Appendix*, Fig. S2 and Movie S6). Δ*pilH* colonies tend to form clusters of cells jamming into each other, forming swirls and comet-like rafts of migrating cells that quickly disperse, thereby inhibiting persistent collective migration (*SI Appendix*, Fig. S2 and Movie S6). As a consequence, the leading edge expands more slowly compared with WT, resulting in smaller colony diameter in twitching stab assays (*SI Appendix*, Fig. S1*A*). These observations could explain the patterns observed at the edge of larger colonies (14, 24). In summary, by controlling reversal rates upon collision, Chp-dependent mechanosensing can optimize *P. aeruginosa* collective motility. Chp provides single *P. aeruginosa* cells with the ability to migrate persistently in one direction and to rapidly change twitching direction. PilG promotes persistent forward motility, driving migration over long distances. PilH enables directional changes particularly useful upon collisions with other bacteria.

To investigate how PilG and PilH control twitching direction, we focused on the distribution of T4P between the two poles of a cell. We imaged *P. aeruginosa* by interferometric scattering microscopy (iSCAT) to quantify T4P at each cell pole and evaluate their distributions. We found that the T4P of WT and Δ*cpdA* were nearly randomly distributed (*SI Appendix*, Fig. S3). In contrast, T4P of Δ*pilGcpdA* were distributed more symmetrically compared with the random distribution and to WT. While Δ*pilH* had too many T4P for a direct comparison with other mutants, we could quantify symmetry in the less-piliated Δ*pilHcyaB* background (*SI Appendix*, Fig. S1*D*). The T4P of Δ*pilHcyaB* were markedly more asymmetrically distributed than WT (*SI Appendix*, Fig. S3), consistent with its inability to reverse twitching direction. We conclude that the Chp system polarizes T4P to regulate twitching direction. PilG promotes unipolar T4P deployment driving persistent forward migration, while PilH promotes T4P deployment at both poles simultaneously, favoring reversals.

T4P extend and retract from the cell surface by respective polymerization and depolymerization of the pilin subunit PilA at the poles. The extension motor PilB assembles PilA monomers to extend T4P, while the retraction motors PilT and PilU disassemble filaments to generate traction forces (Fig. 1*A*) (9, 10). We reasoned that for the Chp system to regulate T4P polarization and set a cell's twitching direction, it must control either extension or retraction at a given pole. To test this hypothesis, we investigated how the localization of extension and retraction motors regulate the deployment of T4P to direct twitching. First, we simultaneously visualized T4P distribution and motor protein subcellular localization within single cells. To this end, we generated chromosomal mNeonGreen (mNG) fluorescent protein fusions at their native loci to the extension motor PilB, to its regulator FimX (25), and to the retraction motors PilT and PilU (Fig. 3*A*). All fusion proteins were functional and exhibited primarily bright fluorescent foci at one or both poles, globally consistent with inducible plasmid-borne fusion proteins, with the exception of PilU, which had been reported as asymmetrically localized but under different imaging, expression, and growth conditions (26, 27). We leveraged correlative iSCAT fluorescence microscopy for simultaneous imaging of T4P and fluorescent reporter fusions (Fig. 3*B*) (28). In single cells, we identified the pole with the brightest fluorescent signal and the pole with most T4P. We then categorized cells into two groups: cells with more T4P at the bright pole versus cells with less T4P at the bright pole. We found that in more than 60% of cells, the poles with more T4P had the brightest PilB-mNG fluorescent signal (Fig. 3*C*) (26). On the other hand, we found no negative correlation between mNG-PilT or mNG-PilU signals and relative numbers of T4P, which would be expected if cells controlled T4P distribution using retraction. We conclude that PilB, but neither PilT nor PilU, control the polarized deployment of T4P.

Since most but not all cells had more T4P at the bright PilB pole, we considered whether PilB controls the direction of twitching migration of single *P. aeruginosa* cells. To test this hypothesis, we investigated the dynamic localization of motors in single twitching cells (*SI Appendix*, Fig. S4 and Movie S7). While mNG-PilT and mNG-PilU fusions were fully functional, PilB-mNG exhibited a partial twitching motility defect (*SI Appendix*, Fig. S5). We therefore systematically validated PilB localization results by the visualization of its regulator FimX using mNG-FimX, which was fully functional (*SI Appendix*, Fig. S5). We tracked single cells while measuring the subcellular localization of the fusion proteins. We first categorized cells as moving and nonmoving. We then measured the proportion of cells that had asymmetric and symmetric protein localizations based on a threshold of fluorescence ratio between poles. We found that PilB-mNG and mNG-FimX localizations were more asymmetric (i.e., polarized) in moving cells

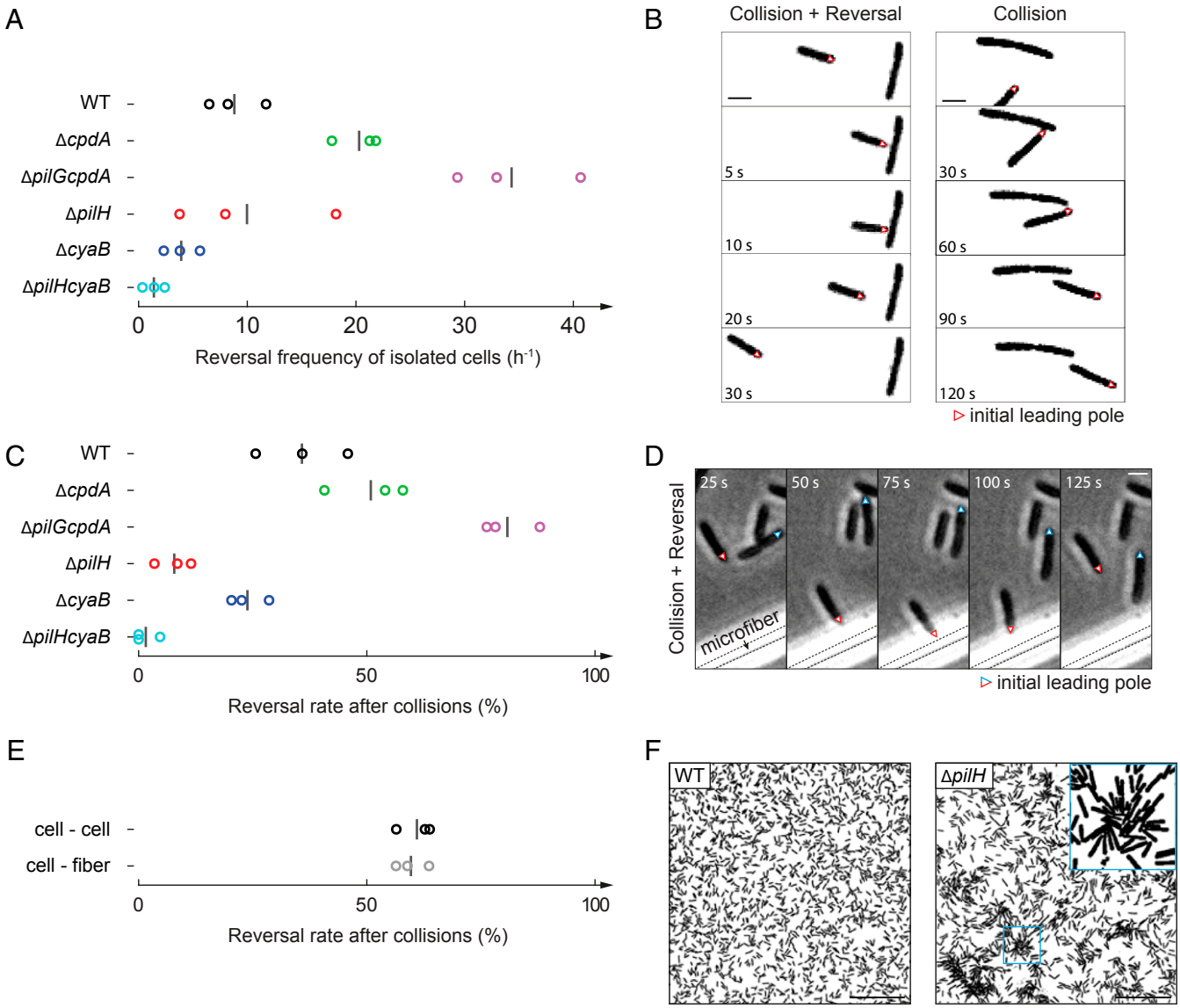

Fig. 2. The Chp system controls reversals of twitching *P. aeruginosa* cells. (*A*) Quantification of reversal rates in Chp and cAMP mutants. Δ*pilGcpdA* has highest reversal frequency. Δ*pilH* has a twofold lower reversal frequency than Δ*cpdA*. Circles correspond to biological replicates, and black bars represent their mean. (*B*) Snapshots of WT reversing upon collision with another cell (*Left*). The same sequence for a Δ*pilH* cell, failing to reverse upon collision (*Right*). The red triangle indicates the initial leading pole of the bacterium. (Scale bar, 2 μm.) (*C*) Fraction of cells reversing upon collision with another cell. About half of WT cells reverse after collision, Δ*pilH* almost never reverses after collision, and Δ*pilGcpdA* almost always reverses. Circles correspond to biological replicates, and black bars represent their mean. (*D*) Phase contrast image sequence of WT cells reversing upon collision with glass microfibers and other cells. The dashed lines indicate the position of the fiber. (Scale bar, 2 μm.) (*E*) Fraction of WT cells reversing upon collision with another cell and with a glass microfiber. A total of 60% of cells reverse after collision, irrespective of the type of obstacle. Circles correspond to biological replicates, and black bars represent their mean. (*F*) While WT is able to move efficiently at high density, the reduced ability of Δ*pilH* to reverse upon collision leads to cell jamming and clustering. (Scale bar, 50 μm.) Background strain: PAO1 Δ*fliC*.

compared with nonmoving cells (Fig. 3*D*). In addition, both fusion proteins changed localization and polarity during reversals (*SI Appendix*, Fig. S6 and Movie S8) (25). In contrast, the localization of mNG-PilT and mNG-PilU was largely symmetric across the population, without marked symmetry differences between nonmoving and moving cells. Since PilB and FimX polarize in moving cells, we computed the correlation between the twitching direction and fusion protein polarization (i.e., the localization of their brightest polar spot). We found that more than 90% of cells moved in the direction of the bright PilB and FimX pole (Fig. 3*E*). Thus, PilB polarization correlates more strongly with motility than with T4P number (Fig. 3*C*). While we measure twitching for minutes over nearly 100 T4P extension and retraction events (29), correlative iSCAT gives a snapshot of the T4P distribution in a given cell, explaining the discrepancy between conditions. Altogether, our data shows that polarized extension and constitutive retraction controls *P. aeruginosa* twitching direction.

The Chp system regulates T4P distribution, which itself is under the control of the PilB polarization. Since T4P and Chp mediate surface sensing to regulate transcription, we hypothesize that mechanosensing also regulates the subsequent extension of additional T4P (19). As a result, we tested whether T4P activity itself regulates PilB polarization. We reasoned that the longer a cell resides on a surface, the more likely it is to experience mechanical stimuli from T4P. We thus compared polarization of cell populations immediately after contact (10 min) with populations

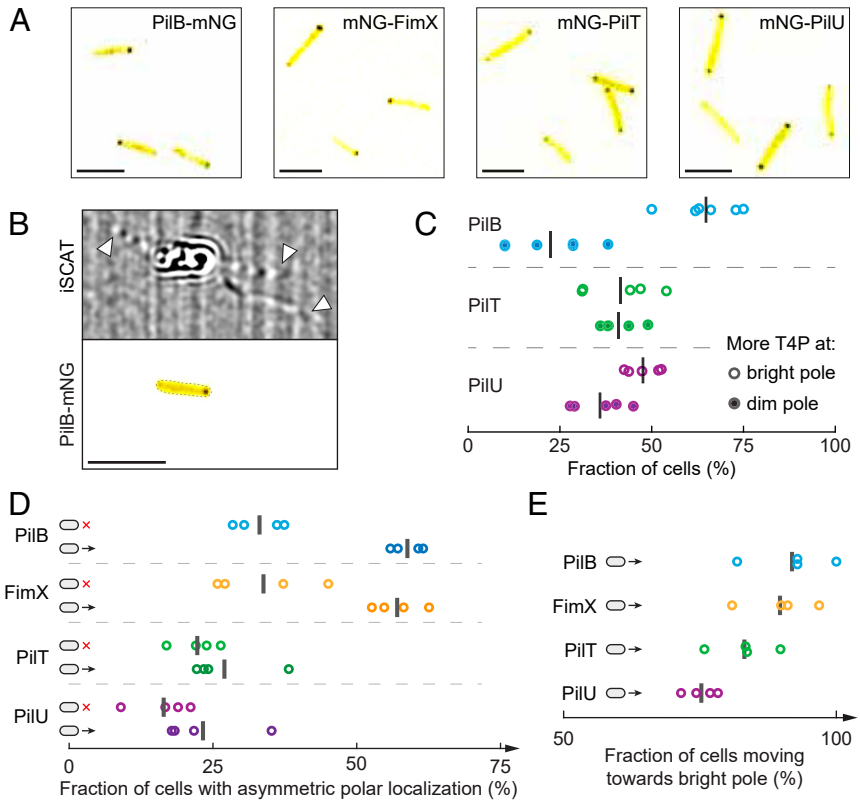

Fig. 3. The localization of the extension motor PilB sets the direction of twitching and the polarization of T4P activity. (*A*) Snapshot of chromosomal fluorescent protein fusions to the extension motor PilB, its regulator FimX, and the retraction motors PilT and PilU. (Scale bars, 5 μm.) (*B*) Simultaneous imaging of PilB-mNG and T4P by correlative iSCAT fluorescence. White arrowheads indicate T4P. (Scale bar, 5 μm.) (*C*) Fraction of cells with more T4P at bright versus dim fluorescent pole. Most cells have more T4P at the bright PilB-mNG pole. We could not distinguish a T4P depletion at the bright retraction motor poles. Each circle is the mean fraction for one biological replicate. Black bars correspond to their mean across replicates. (*D*) Comparison of the symmetry of polar fluorescence between moving and nonmoving cells. PilB and FimX signal is more asymmetric in moving cells, which is not the case for PilT and PilU. (*E*) Fraction of cells twitching in the direction of their brightest pole. Circles correspond the fraction of each biological replicate, and black bars represent their mean.

that were associated with the surface for longer times (60 min). We focused on the dynamic localization of mNG-FimX. First, we found that in many cells, polar mNG-FimX foci relocated from pole to pole within a short timeframe after surface contact as if they were oscillating (Fig. 4*A* and Movie S9). These observations were reminiscent of oscillations in the twitching and gliding regulators observed in *M. xanthus* (23, 30, 31). The proportion of cells exhibiting these oscillations became smaller after prolonged surface contact (Fig. 4*B* and *SI Appendix*, Fig. S7*A*), suggesting that surface sensing inhibits mNG-FimX oscillations and stabilizes polarization. To test whether mechanosensing with T4P induces polarization of the extension machinery, we visualized mNG-FimX in a Δ*pilA* mutant background, which also displayed oscillations (Fig. 4*C* and Movie S10). We found that the fraction of Δ*pilA* cells that showed mNG-FimX oscillations 10 and 60 min after surface contact were equal, near 90% (Fig. 4*D*). The distributions of oscillation frequencies between these two states were also indistinguishable (*SI Appendix*, Fig. S7*B*). Altogether, our results demonstrate that T4P-mediated mechanosensing at one pole locally recruits and stabilizes extension motors, thereby inducing a positive feedback onto their own activity. While several exogenous molecular compounds bias collective or single-cell twitching migration (15–18), our data shows chemical gradients are not necessary for the active regulation of twitching.

PilB polarization sets the twitching direction of single cells, and PilG and PilH regulate T4P polarization to control reversals. We therefore investigated how the Chp system regulates PilB localization to control a cell's direction of motion. We compared the mean localization profiles of PilB-mNG and mNG-FimX in WT, Δ*pilG*, and Δ*pilH* backgrounds (Fig. 5 *A* and *B* and *SI Appendix*, Fig. S8*A*). Both fusion proteins had greater polar fluorescent signal in Δ*pilH* and lower polar signal in Δ*pilG* compared with WT (Fig. 5 *C* and *D*). We computed a polar localization index, which measures the proportion of the signal localized at the poles relative to the total fluorescence (*SI Appendix*, Fig. S8*B*). About 50% of the mNG-FimX and PilB-mNG signal is found at the poles for WT, 70% of the signal is polar in Δ*pilH*, and most of the signal is diffuse in Δ*pilG* (Fig. 5 *E* and *G*). We next computed a symmetry index that quantifies the extent of signal polarization, that is, how bright a pole is compared with the other, with a value of 0.5 being completely symmetric (*SI Appendix*, Fig. S8*B*). WT cells grown in liquid had a mNG-FimX and PilB-mNG symmetry index of about 0.6 (Fig. 5 *F* and *H*). In contrast, Δ*pilH* cells were more polarized, with a symmetry index close to 0.75. Compared with WT, mNG-FimX was more symmetric in a Δ*pilG* background (Fig. 5*H*). We verified that the increase in expression levels in the different Chp mutants did not exacerbate PilB and FimX localization and polarization (*SI Appendix*, Fig. S9). In summary, we showed that PilG promotes polar recruitment and polarization of PilB and its regulator FimX, which is counteracted by PilH.

We then wondered how *P. aeruginosa* orchestrates two response regulators with opposing functions. Yeast and amoebae control cell polarization in response to environmental cues using spatially structured positive and negative feedback (32). By analogy, we considered a model wherein PilG and PilH segregate to implement

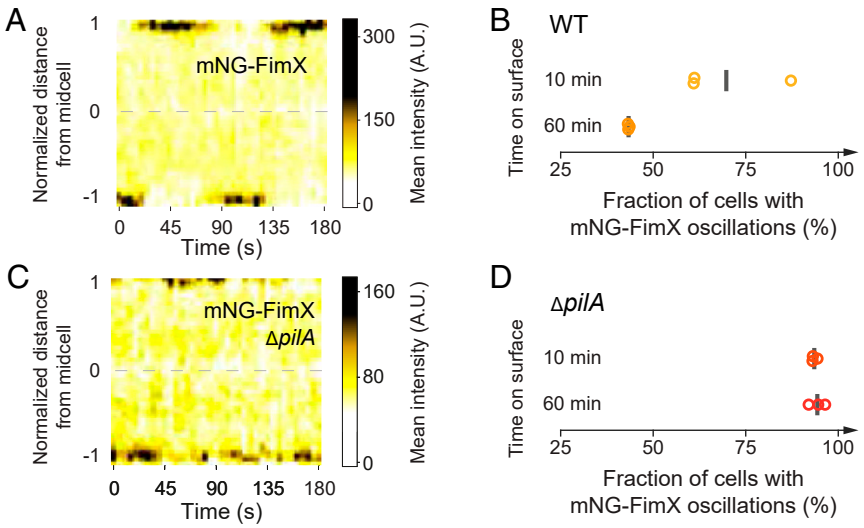

Fig. 4. Mechanical input signal from T4P controls the polarization of FimX, the activator of the extension motor PilB. (*A*) Kymograph of mNG-FimX fluorescence in a nonmoving cell 10 min after surface contact. The bright fluorescent focus sequentially disappears from one pole to appear at the opposite to establish oscillations. (*B*) Fraction of cells that showed pole to pole oscillations in WT and Δ*pilA*. The proportion of oscillating WT reduces as they remain on the surface, conversely increasing the proportion of stably polarized cells. (*C*) Kymograph of mNG-FimX fluorescence in a Δ*pilA* background 60 min after surface contact. (Scale bar, 5 μm.) (*D*) Most Δ*pilA* cells maintain oscillatory fluctuations in mNG-FimX polar localization.

positive and negative feedback at distinct subcellular locations (33). We therefore investigated the localization of functional mNG-PilG and mNG-PilH integrated at their native chromosomal loci (Fig. 6*A*). We found that PilG predominantly localizes to the poles (Fig. 6 *B* and *C*). In contrast, PilH is mainly diffused in the cytoplasm, with only a small fraction at the poles (Fig. 6 *B* and *C*). *P. aeruginosa* can therefore ensure the antagonistic functions of PilG and PilH by localizing the former to the poles and the latter to the cytoplasm.

We next analyzed the relationship between a cell's direction of migration with mNG-PilG and mNG-PilH polarization (*SI Appendix*, Fig. S10*A* and Movie S11). We found that 90% of cells moved toward their bright mNG-PilG pole, while only 50% moved toward their bright mNG-PilH, corresponding to a random orientation relative to the direction of migration (Fig. 6*D*). By comparing the asymmetry of polar foci, we found that mNG-PilG signal was largely asymmetric in motile cells compared with the nonmotile population (Fig. 6*E*). Correlative iSCAT fluorescence highlighted that the brightest mNG-PilG polar spots had more T4P (Fig. 6*F*). Consistent with this finding, in cells that reversed twitching direction, mNG-PilG localization switched to the new leading pole prior to reversal (*SI Appendix*, Fig. S10*B* and Movie S12). We found that the polar signal of mNG-PilH was mainly symmetric, both in moving and nonmoving subpopulations (Fig. 6*D*). Thus, PilG, but not PilH, actively localizes to the leading pole during twitching, recapitulating the dynamic polarization of PilB and FimX. We confirmed this by imaging the double fluorescent protein fusions mScarlet-I-PilG with mNG-FimX and mScarlet-I-PilG with PilB-mNG (*SI Appendix*, Figs. S11 and S12*A*). In both strains, the FimX/PilB and PilG colocalized at the leading pole of twitching cells (*SI Appendix*, Fig. S12*B*) and changed polarization upon reversals (*SI Appendix*, Fig. S12 *C–F*). We could not, however, distinguish the order at which FimX and PilG changed polarity during reversals, nor could we measure differences in the delay between motility reversal and polarity changes in single fusions (*SI Appendix*, Fig. S13). Therefore, T4P input at the leading pole activates PilG. Polar PilG rapidly drives a local positive feedback on T4P extension to maintain the direction of twitching. Cytoplasmic PilH stimulate reversals by inhibiting PilB polarization, permitting reassembly at the opposite pole. In summary, *P. aeruginosa* controls mechanotactic twitching using a local-excitation, global-inhibition signaling network architecture akin to chemotactic signaling in amoebae and neutrophils (*SI Appendix*, Fig. S14) (5, 34).

Discussion

We discovered that *P. aeruginosa* controls the direction of twitching motility in response to mechanical signals through the motility machinery itself. This migration strategy differs from the one employed in chemotactic control of swimming motility. Chemotaxis systems control the rate at which swimming cells switch the direction of rotation of their flagella, generating successive run and tumbles (4, 21) or flicks (35) that cause directional changes. However, T4P must disassemble from one pole and reassemble at the opposite in order to reverse cell movement. In essence, this tactic strategy is akin to the one of single eukaryotic cells such as amoebae and neutrophils that locally remodel their cytoskeleton to attach membrane protrusions in the direction of a stimulus (5). *P. aeruginosa* twitching direction is also biased by chemical gradients, suggesting that Chp also senses chemical stimuli (15–18). Our results do not disprove that Chp controls twitching chemotactically but provide a complementary perspective on these observations. In one scenario, a strong chemical gradient could produce a gradient in surface chemistry that causes differential adhesion of T4P between leading and lagging poles, inducing a bias in twitching direction. The relative contributions of chemical and mechanical inputs in activating the Chp system will therefore require further biophysical investigations.

Ultimately, the ability to balance persistent forward migration with reversals optimizes *P. aeruginosa* individual twitching. Reversal may occur spontaneously or upon perturbations, for example, when colliding another cell. The Chp system may also promote asymmetric piliation of upright twitching *P. aeruginosa* cells during exploratory motility (36). We also found that the ability to reverse upon collision prevents the jamming of groups of cells, supporting a model wherein the Chp system orchestrates collective migration (13). More generally, we anticipate that other bacteria, as well as archaeal and eukaryotic species that actively migrate on surfaces, leverage mechanosensation to control reversal rates and orchestrate collective motility behaviors (31).

Bacteria use dedicated sensing systems to regulate gene expression and adhesion in response to mechanical signals (3, 37–39). Beyond bacteria, eukaryotic cells also transduce mechanical signals

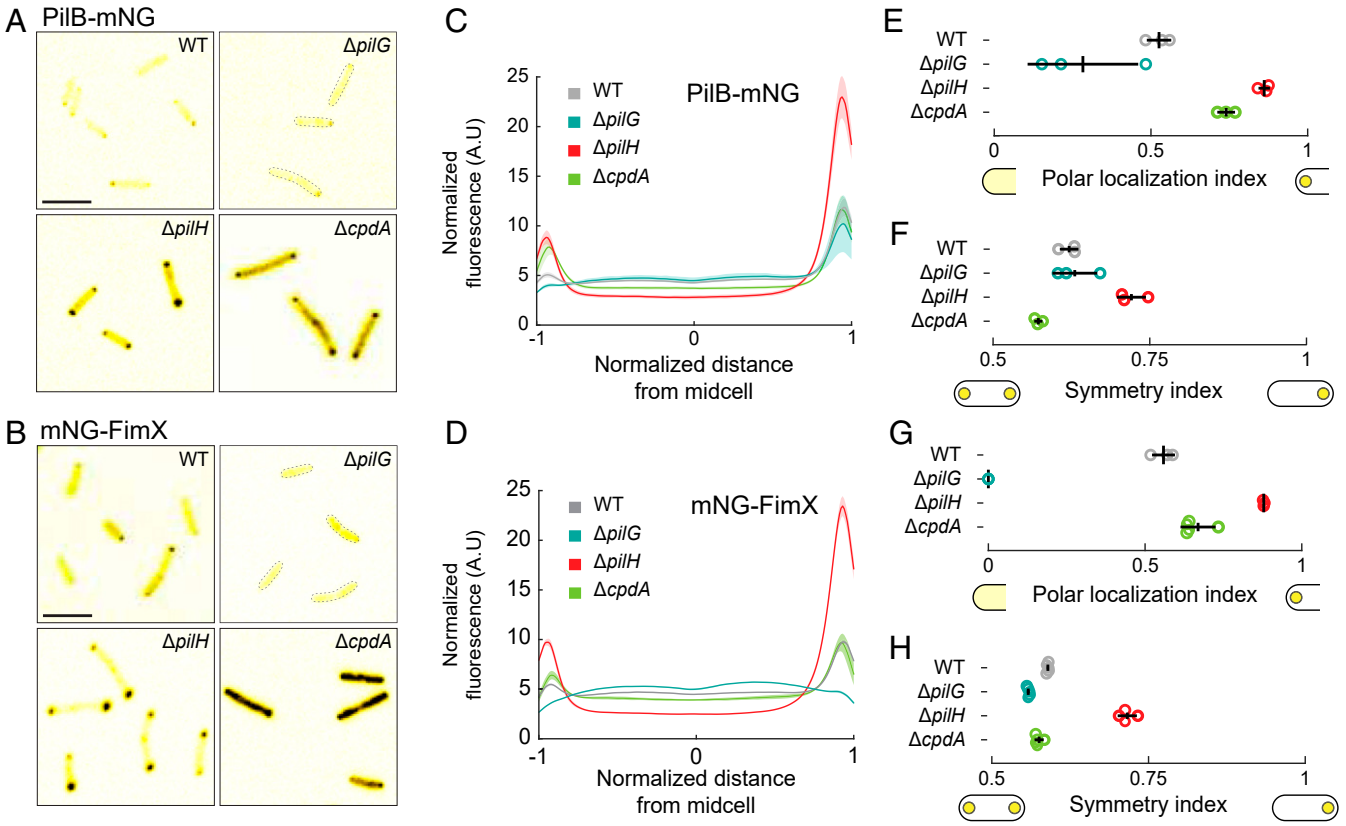

Fig. 5. PilG and PilH control the polarization of T4P extension machinery. Snapshots of PilB-mNG (*A*) and mNG-FimX (*B*) fluorescence in WT, Δ*pilG*, Δ*pilH*, and Δ*cpdA* background. (Scale bar, 5 μm.) (*C* and *D*) Normalized fluorescence profiles along the major cell axis of the motor protein PilB and its activator FimX (*SI Appendix*, Fig. S8*A*). Solid lines represent the mean normalized fluorescence profiles across biological replicates. The shaded area represents SD across biological replicates. (*E* and *G*) Polar localization index of PilB-mNG and mNG-FimX respectively, quantifying the extent of polar signal compared with a diffused configuration (*SI Appendix*, Fig. S8*B*). An index of 0 and 1 respectively correspond to completely diffuse and polar signals. Relative to WT and Δ*cpdA*, polar localization is higher in Δ*pilH* and lower in in Δ*pilG*. (*F* and *H*) Symmetry index of PilB-mNG and mNG-FimX, respectively, representing the ratio of the brightest pole fluorescence to the total polar fluorescence. The values 0.5 and 1 respectively correspond to a symmetric bipolar and a unipolar localization. Δ*pilH* has higher symmetry index than WT and Δ*cpdA*. Circles represent the median of each biological replicate. Black bars represent (vertical) mean and (horizontal) SD across biological replicates.

into cellular responses, regulating an array of physiological processes including development, immunity, and touch sensation (40). Eukaryotic cell motility is also sensitive to mechanical cues. For example, adherent mammalian cells migrate up gradients of substrate material stiffness in a process termed durotaxis (41). We established that single cells can actively sense their mechanical environment to control motility on the timescale of seconds. Our work thus expands the panel of signals activating bacterial sensing systems and more generally highlights the role of mechanics in regulating motility, be it in bacteria, archaea, or eukaryotes (42).

Altogether, Chp functions as a spatial sensor for mechanical input. Thus, chemotaxis-like systems can sense spatially resolved mechanical signals, a feat that is still debated when only considering diffusible molecules as input stimuli (43). Phototactic systems may, however, be an exception by conferring cyanobacteria the ability to spatially sense gradients of light (44, 45). Accordingly, the Pix phototactic system of the cyanobacterium *Synechocystis* shares signal transduction architecture with the *P. aeruginosa* Chp system by harboring two CheY-like response regulators, PixG and PixH (44, 45). There also exists a broad range of chemotaxis-like systems with even higher degrees of architectural complexity (46). We thus highlight that their subcellular arrangement may play important functions in the mechanism by which they regulate motility.

Finally, we revealed an unexpected commonality between bacteria and single eukaryotic cells in the way they transduce environmental signals to control polarity (5). Amoebae and neutrophils harness complex circuitry which combines positive and negative feedback loops to chemotax (32). Positive regulators activate actin polymerization locally to drive membrane protrusion in the direction of polarization. Negative regulators inhibit actin polymerization throughout the cytoplasm to limit directional changes while also permitting adaptation (32). Altogether, these cells establish a local activation global-inhibition landscape that balances directional persistence with adaptation (34). By virtue of PilG and PilH compartmentalization, *P. aeruginosa* replicates the local activation global-inhibition landscape (34). We have therefore uncovered a signal transduction principle permitting mechanotaxis in response to spatially resolved signals that is conserved across kingdoms of life.

Materials and Methods

Bacterial Strains and Growth Conditions. All strains used in this study are listed in *SI Appendix*, Table S1. The *P. aeruginosa* strain used was PAO1 strain ATCC 15692 (American Type Culture Collection). *E. coli* strain DH5α was used for vector construction, and *E. coli* strain S17.1 was used for the conjugation of vectors into *P. aeruginosa*. All bacterial strains were grown in Luria–Bertani (LB) medium (Carl Roth) at 37 °C with 290 rpm shaking. Regular solid LB media were prepared by adding 1.5% (wt · vol^{-1}) agar (Fisher Bioreagents). Additional information on media and strain construction are given in *SI Appendix*.

Phase Contrast and Fluorescence Microscopy. Microscopy was performed on an inverted Nikon TiE epifluorescence microscope controlled with NIS-Elements (version AR 5.02.03). Specific experimental procedures are given in *SI Appendix*. For pure phase contrast microscopy, a 40× Plan APO NA 0.9 phase contrast objective was used. For fluorescence microscopy, a 100× Plan

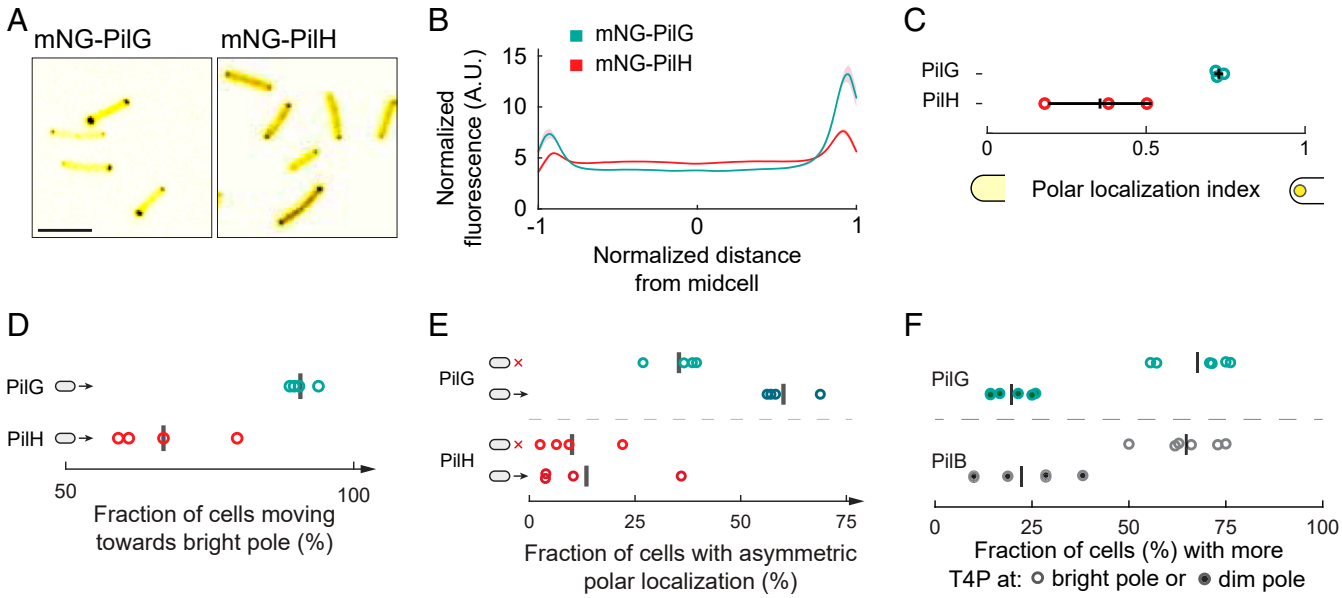

Fig. 6. PilG and PilH dynamic localization establish a local-excitation, global-inhibition signaling landscape. (*A*) Snapshots of mNG-PilG and mNG-PilH fluorescence. (Scale bar, 5 μm.) (*B*) Comparison of mNG-PilG and mNG-PilH normalized mean fluorescent profiles. (*C*) The polar localization index of mNG-PilG is relatively large showing PilG is mostly polar. In contrast, mNG-PilH has a low polar localization index and is thus mostly cytoplasmic. Circles represent the median of each biological replicate. Black bars represent the (vertical) mean and (horizontal) SD across biological replicates. (*D*) Protein polarization relative to the twitching direction. Cells predominantly move toward the brighter mNG-PilG pole. The fraction for mNG-PilH is close to 50%, corresponding to a random polarization relative to the direction of motion. Black bars represent the mean across biological replicates. (*E*) Comparison of the symmetry of the polar fluorescent foci of moving cells with nonmoving cells for mNG-PilG and mNG-PilH fusion proteins. There is an enrichment for mNG-PilG polar asymmetry in moving cells but no differences in mNG-PilH. Black bars represent the mean across biological replicates. (*F*) Fraction of cells with more T4P at bright versus dim mNG-PilG fluorescent pole. Most cells have more T4P at the bright mNG-PilG pole, similar to PilB (data from Fig. 3*C* in gray as reference). Each circle is the mean fraction for one biological replicate. Black bars correspond to their mean across replicates.

APO NA 1.45 phase contrast oil objective and Semrock YFP-2427B or TxRed-A-Basic-NTE filters were used as needed.

Experimental Procedures and Analysis. An extended description of experimental procedures and analysis methods, including analysis of twitching motility and localization of fluorescent protein fusions, are given in detail in *SI Appendix*.

Data Availability. All data and ImageJ, Python, and MATLAB codes are available on GitHub under the following repository: https://github.com/PersatLab/Mechanotaxis.git. Raw images are available from the corresponding authors upon request.

ACKNOWLEDGMENTS. L.T., Z.A.-M., I.V., X.P., and A.P. are supported by Swiss National Science Foundation Project Grant 310030_189084. M.J.K. is supported by European Molecular Biology Organization postdoctoral fellowship (ALTF 495-2020). J.N.E., Y.F.I., R.P., and H.M. are supported by NIH R01 Grant AI129547 and by the Cystic Fibrosis Foundation Grant 495008.

1. J. W. Costerton, Z. Lewandowski, D. E. Caldwell, D. R. Korber, H. M. Lappin-Scott, Microbial biofilms. *Annu. Rev. Microbiol.* **49**, 711–745 (1995).
2. K. F. Jarrell, M. J. McBride, The surprisingly diverse ways that prokaryotes move. *Nat. Rev. Microbiol.* **6**, 466–476 (2008).
3. Y. F. Dufrêne, A. Persat, Mechanomicrobiology: How bacteria sense and respond to forces. *Nat. Rev. Microbiol.* **18**, 227–240 (2020).
4. S. Bi, V. Sourjik, Stimulus sensing and signal processing in bacterial chemotaxis. *Curr. Opin. Microbiol.* **45**, 22–29 (2018).
5. P. J. M. Van Haastert, P. N. Devreotes, Chemotaxis: Signalling the way forward. *Nat. Rev. Mol. Cell Biol.* **5**, 626–634 (2004).
6. A. M. Stock, V. L. Robinson, P. N. Goudreau, Two-component signal transduction. *Annu. Rev. Biochem.* **69**, 183–215 (2000).
7. M. A. Matilla, T. Krell, The effect of bacterial chemotaxis on host infection and pathogenicity. *FEMS Microbiol. Rev.* **42**, fux052 (2018).
8. S. L. Porter, G. H. Wadhams, J. P. Armitage, *Rhodobacter sphaeroides*: Complexity in chemotactic signalling. *Trends Microbiol.* **16**, 251–260 (2008).
9. L. L. Burrows, *Pseudomonas aeruginosa* twitching motility: Type IV pili in action. *Annu. Rev. Microbiol.* **66**, 493–520 (2012).
10. A. J. Merz, M. So, M. P. Sheetz, Pilus retraction powers bacterial twitching motility. *Nature* **407**, 98–102 (2000).
11. J. J. Bertrand, J. T. West, J. N. Engel, Genetic analysis of the regulation of type IV pilus function by the Chp chemosensory system of *Pseudomonas aeruginosa*. *J. Bacteriol.* **192**, 994–1010 (2010).
12. N. B. Fulcher, P. M. Holliday, E. Klem, M. J. Cann, M. C. Wolfgang, The *Pseudomonas aeruginosa* Chp chemosensory system regulates intracellular cAMP levels by modulating adenylate cyclase activity. *Mol. Microbiol.* **76**, 889–904 (2010).
13. C. B. Whitchurch *et al.*, Characterization of a complex chemosensory signal transduction system which controls twitching motility in *Pseudomonas aeruginosa*. *Mol. Microbiol.* **52**, 873–893 (2004).
14. A. Darzins, Characterization of a *Pseudomonas aeruginosa* gene cluster involved in pilus biosynthesis and twitching motility: Sequence similarity to the chemotaxis proteins of enterics and the gliding bacterium *Myxococcus xanthus*. *Mol. Microbiol.* **11**, 137–153 (1994).
15. D. B. Kearns, J. Robinson, L. J. Shimkets, *Pseudomonas aeruginosa* exhibits directed twitching motility up phosphatidylethanolamine gradients. *J. Bacteriol.* **183**, 763–767 (2001).
16. D. H. Limoli *et al.*, Interspecies interactions induce exploratory motility in *Pseudomonas aeruginosa*. *eLife* **8**, e47365 (2019).
17. N. M. Oliveira, K. R. Foster, W. M. Durham, Single-cell twitching chemotaxis in developing biofilms. *Proc. Natl. Acad. Sci. U.S.A.* **113**, 6532–6537 (2016).
18. L. M. Nolan, L. C. McCaughey, J. Merjane, L. Turnbull, C. B. Whitchurch, ChpC controls twitching motility-mediated expansion of *Pseudomonas aeruginosa* biofilms in response to serum albumin, mucin and oligopeptides. *Microbiology (Reading)* **166**, 669–678 (2020).
19. A. Persat, Y. F. Inclan, J. N. Engel, H. A. Stone, Z. Gitai, Type IV pili mechanochemically regulate virulence factors in *Pseudomonas aeruginosa*. *Proc. Natl. Acad. Sci. U.S.A.* **112**, 7563–7568 (2015).
20. R. N. C. Buensuceso *et al.*, Cyclic AMP-independent control of twitching motility in *Pseudomonas aeruginosa*. *J. Bacteriol.* **199**, e00188-17 (2017).
21. H. C. Berg, "Chapter 9. Behavioral Hardware" in *E. coli in Motion*, E. Greenbaum, Ed. (Springer-Verlag, New York, NY, 2004), pp. 77–90.
22. S. Thutupalli, M. Sun, F. Bunyak, K. Palaniappan, J. W. Shaevitz, Directional reversals enable *Myxococcus xanthus* cells to produce collective one-dimensional streams during fruiting-body formation. *J. R. Soc. Interface* **12**, 20150049 (2015).
23. B. D. Blackhart, D. R. Zusman, "Frizzy" genes of *Myxococcus xanthus* are involved in control of frequency of reversal of gliding motility. *Proc. Natl. Acad. Sci. U.S.A.* **82**, 8767–8770 (1985).

24. O. J. Meacock, A. Doostmohammadi, K. R. Foster, J. M. Yeomans, W. M. Durham, Bacteria solve the problem of crowding by moving slowly. *Nat. Phys.* **17**, 205–210 (2021).
25. R. Jain, O. Sliusarenko, B. I. Kazmierczak, Interaction of the cyclic-di-GMP binding protein FimX and the Type 4 pilus assembly ATPase promotes pilus assembly. *PLoS Pathog.* **13**, e1006594 (2017).
26. P. Chiang, M. Habash, L. L. Burrows, Disparate subcellular localization patterns of *Pseudomonas aeruginosa* Type IV pilus ATPases involved in twitching motility. *J. Bacteriol.* **187**, 829–839 (2005).
27. B. I. Kazmierczak, M. B. Lebron, T. S. Murray, Analysis of FimX, a phosphodiesterase that governs twitching motility in *Pseudomonas aeruginosa*. *Mol. Microbiol.* **60**, 1026–1043 (2006).
28. J. Ortega Arroyo, D. Cole, P. Kukura, Interferometric scattering microscopy and its combination with single-molecule fluorescence imaging. *Nat. Protoc.* **11**, 617–633 (2016).
29. L. Talà, A. Fineberg, P. Kukura, A. Persat, *Pseudomonas aeruginosa* orchestrates twitching motility by sequential control of type IV pili movements. *Nat. Microbiol.* **4**, 774–780 (2019).
30. C. Galicia *et al*., MglA functions as a three-state GTPase to control movement reversals of *Myxococcus xanthus*. *Nat. Commun.* **10**, 5300 (2019).
31. M. Guzzo *et al*., A gated relaxation oscillator mediated by FrzX controls morphogenetic movements in *Myxococcus xanthus*. *Nat. Microbiol.* **3**, 948–959 (2018).
32. O. Brandman, T. Meyer, Feedback loops shape cellular signals in space and time. *Science* **322**, 390–395 (2008).
33. Y. F. Inclan *et al*., A scaffold protein connects type IV pili with the Chp chemosensory system to mediate activation of virulence signaling in *Pseudomonas aeruginosa*. *Mol. Microbiol.* **101**, 590–605 (2016).
34. A. Levchenko, P. A. Iglesias, Models of eukaryotic gradient sensing: Application to chemotaxis of amoebae and neutrophils. *Biophys. J.* **82**, 50–63 (2002).
35. K. Son, J. S. Guasto, R. Stocker, Bacteria can exploit a flagellar buckling instability to change direction. *Nat. Phys.* **9**, 494–498 (2013).
36. M. L. Gibiansky *et al*., Bacteria use type IV pili to walk upright and detach from surfaces. *Science* **330**, 197 (2010).
37. I. Hug, S. Deshpande, K. S. Sprecher, T. Pfohl, U. Jenal, Second messenger-mediated tactile response by a bacterial rotary motor. *Science* **358**, 531–534 (2017).
38. C. K. Ellison *et al*., Obstruction of pilus retraction stimulates bacterial surface sensing. *Science* **358**, 535–538 (2017).
39. J. E. Sanfilippo *et al*., Microfluidic-based transcriptomics reveal force-independent bacterial rheosensing. *Nat. Microbiol.* **4**, 1274–1281 (2019).
40. J. M. Kefauver, A. B. Ward, A. Patapoutian, Discoveries in structure and physiology of mechanically activated ion channels. *Nature* **587**, 567–576 (2020).
41. R. Sunyer *et al*., Collective cell durotaxis emerges from long-range intercellular force transmission. *Science* **353**, 1157–1161 (2016).
42. A. R. Houk *et al*., Membrane tension maintains cell polarity by confining signals to the leading edge during neutrophil migration. *Cell* **148**, 175–188 (2012).
43. H. C. Berg, E. M. Purcell, Physics of chemoreception. *Biophys. J.* **20**, 193–219 (1977).
44. N. Schuergers *et al*., Cyanobacteria use micro-optics to sense light direction. *eLife* **5**, 1–16 (2016).
45. N. Schuergers, C. W. Mullineaux, A. Wilde, Cyanobacteria in motion. *Curr. Opin. Plant Biol.* **37**, 109–115 (2017).
46. S. L. Porter, G. H. Wadhams, J. P. Armitage, Signal processing in complex chemotaxis pathways. *Nat. Rev. Microbiol.* **9**, 153–165 (2011).